FOUNDATIONS
ADVANCES

ISSN: 2053-2733
journals.iucr.org/a

A study of X-ray multiple diffraction by means of section topography

V. G. Kohn and I. A. Smirnova

Acta Cryst. (2015). A**71**, 519–525

Acta Cryst A FOUNDATIONS ADVANCES

ISSN 2053-2733

A study of X-ray multiple diffraction by means of section topography

V. G. Kohn[a]* and I. A. Smirnova[b]

[a]National Research Centre 'Kurchatov Institute', 123182 Moscow, Russian Federation, and [b]Institute of Solid State Physics RAS, 142432 Chernogolovka, Moscow district, Russian Federation. *Correspondence e-mail: kohnvict@yandex.ru

Received 6 May 2015
Accepted 24 June 2015

Edited by L. D. Marks, Northwestern University, USA

Keywords: X-ray diffraction; section topography; multiple diffraction; computer simulations; laboratory study.

The results of theoretical and experimental study are presented for the question of how the X-ray multiple diffraction in a silicon single crystal influences the interference fringes of section topography for the 400 reflection in the Laue case. Two different cases of multiple diffraction are discovered for zero and very small values of the azimuthal angle for the sample in the form of a plate with the surface normal to the 001 direction. The cases are seen on the same topogram without rotation of the crystal. Accurate computer simulations of the section topogram for the case of X-ray multiple diffraction are performed for the first time. It is shown that the structure of interference fringes on the section topogram in the region of multiple diffraction becomes more complicated. It has a very sharp dependence on the azimuthal angle. The experiment is carried out using a laboratory source under conditions of low resolution over the azimuthal angle. Nevertheless, the characteristic inclination of the interference fringes on the tails of the multiple diffraction region is easily seen. This phenomenon corresponds completely to the computer simulations.

1. Introduction

The equations which describe the phenomenon of multiple diffraction of the X-ray plane monochromatic wave on the three-dimensional single-crystal lattice were derived by Ewald in 1917 (Authier, 2005; Chang, 2004; Pinsker, 1978). However, detailed study of the phenomenon itself both experimentally and theoretically only became possible many years later. Indeed, computer calculations are necessary for the accurate solution of the equations, and single crystals of large thickness have to be used in experiments.

In the first experimental works the Renninger experimental setup was widely used (Renninger, 1937) in which one basically considers the diffraction of a nearly parallel and monochromatic wave in the symmetric Bragg case when the diffraction reciprocal-lattice vector is normal to the crystal plate surface, and the beam is reflected from the thin subsurface layer. During rotation of the crystal in the surface plane the polar angle, which is equal to the Bragg angle, stays the same, and the condition of two-beam diffraction is conserved.

At some values of the rotation angle (azimuthal angle) the multiple diffraction conditions become fulfilled. This immediately leads to a decrease in the registered reflection intensity if it is large. If the reflection is forbidden, then initially its intensity equals zero, but under the multiple diffraction conditions one can observe the intensity peak. It is important that such a scheme does not demand a high degree of monochromaticity and collimation of the incident X-ray beam for registering the fact of the phenomenon's existence.

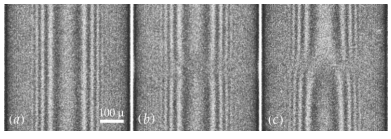

Meanwhile, for the detailed study of peculiarities of angular dependence of the plane-wave reflection, particularly for the study of the effect of total reflection of the forbidden reflected beam (Kon, 1988*a*,*b*), it is necessary to use the almost ideal plane and monochromatic wave, that was achieved experimentally only recently (Kazimirov & Kohn, 2010, 2011; Kohn & Kazimirov, 2012).

In the Laue case, when all beams are transmitted through the crystal and go out the crystal from the other surface, the crystal thickness becomes important. The Borrmann effect is known (Authier, 2005; Chang, 2004; Pinsker, 1978), when part of the radiation is absorbed very slightly and can be registered even for relatively thick crystals. Under the conditions of multiple diffraction a decrease of the absorption coefficient μ by a factor 10^{-4} can occur (Afanas'ev & Kohn, 1977*a*) instead of 0.04 in the two-beam case.

If the crystal plate thickness t is small so that $\mu t < 1$, then the interference between two fields with different absorption coefficients leads to oscillations with a small period on the curve of the angular dependence of the reflection, and it is difficult to study experimentally. Moreover, in this case the diffraction vector is parallel to the crystal surface, and therefore a rotation of the crystal changes the crystal effective thickness.

In the Laue case the method of section topography (Kato & Lang, 1959) is widely used, when the incident beam is restricted by the narrow slit located in front of the crystal. In such a setup only the restricted area inside the Borrmann fan (triangle) is illuminated in the crystal. In the middle of the Borrmann fan the intensity oscillations have a large period. Correspondingly, these fringes are easy to observe even for relatively modest experimental conditions.

In a perfect single crystal the two-beam interference fringes are independent of an azimuthal angle. The local crystal structure defects, for example, individual dislocations, disturb the normal picture of interference fringes and can be detected. However, even in the perfect crystal a disturbance of the fringe picture is possible, if the conditions for the multiple diffraction arise at some values of the azimuthal angle.

Such a disturbance has been observed by Heyroth *et al.* (1999) where the crystal was rotated at the necessary angle. In this work the fringe disturbance was described by means of the method of renormalization of the two-beam diffraction parameter. This renormalization arises in the area where the Bragg conditions for the additional reflection are poorly fulfilled, *i.e.* far from the multiple diffraction point in the angular plane. The theory of such renormalization was first presented by Høier & Marthinsen (1983). The accurate computer simulations were absent.

We note that historically the first evidence of the influence of multiple diffraction on *Pendellösung* fringes of X-ray topography was presented by Hart & Lang (1961). However, in this work a wedge-shaped crystal was used in the case of plane-wave topography, *i.e.* without a narrow slit in front of the crystal. A similar study was presented later in the work by Høier & Aanestad (1981) where computer simulations were performed for the thickness-dependent interference fringes.

It is shown in the present paper that the multiple diffraction disturbance of the interference fringes of section topography can be observed without a rotation of the crystal. Moreover, it is possible to observe several different multiple diffraction cases on the same topogram if the geometry of the experiment and a structure of the crystal are chosen correctly.

Accurate computer simulations of the section topogram in the multiple diffraction area are performed for the first time. We start from the calculation of two-dimensional angular dependence (polar and azimuthal angles) of selected reflected beam intensity under the conditions of multiple diffraction. Then we perform a Fourier transformation for the polar angle. It corresponds to the case of a point source on the entrance surface of the crystal, *i.e.* to the theory of two-wave spherical wave diffraction by Kato (1961). In experiments such a case is performed by means of a narrow slit in front of the crystal. The width of the slit must be much less than the crystal thickness.

The method of calculation is presented in the next section. In §3 the results of computer simulations are discussed. In §4 the experimental setup is described and the experimental results are presented.

2. The method of computer simulations

Let us consider a silicon single crystal with the surface normal to the direction $\mathbf{n}_0 = (0, 0, 1)$ of the crystal lattice (the Z axis of the Cartesian coordinate system). The section topogram is registered for the reflection $(4, 0, 0)$. We choose the direction $(1, 0, 0)$ as the X axis. Then the interference fringes are oriented along the direction $(0, 1, 0)$ (Y axis). If an angular size of the source in the plane YZ is less than 10^{-4} rad, then various segments along the interference fringes will be correspondent to various values of the azimuthal angle $\varphi = y/L$, where L is the distance from the source to the detector.

To realize a two-beam diffraction on the vector $\mathbf{h} = h(1, 0, 0)$ for the considered coordinate system, the incident wavevector has to have the coordinates $\mathbf{k}_0 = K(-\sin\theta, \cos\theta\sin\varphi, \cos\theta\cos\varphi)$, where $h = 8\pi/a$, a is the crystal lattice constant, $K = 2\pi/\lambda$, λ is the radiation wavelength, $\sin\theta = h/2K = 2\lambda/a$. In our case the angle θ is equal to the Bragg angle for the reflection $(4, 0, 0)$.

The geometrical task of searching for additional reflections of multi-wave cases consists of testing all reciprocal-lattice vectors with the Miller indices (n_1, n_2, n_3) for a fulfilment of the Bragg condition for the given direction of the incident wave. This condition can be written as:

$$\begin{aligned} &\alpha = (S_x^2 + S_y^2 + S_z^2 - 1) < 10^{-5}, \\ &S_x = -\sin\theta + An_1, \quad S_y = \cos\theta\sin\varphi + An_2, \\ &S_z = \cos\theta\cos\varphi + An_3 \end{aligned} \tag{1}$$

where $A = \lambda/a$, n_1, n_2, n_3 are integer values. For the silicon crystal it is necessary to consider only even–even or odd–odd combinations.

It is easy to see that the vector $(4, 0, 0)$ satisfies the condition for any value of wavelength and any value of the angle φ.

If $\varphi = 0$, then the vectors $(2, 2, 0)$, $(2, -2, 0)$ satisfy the condition for any values of wavelength too. This case is called a systematic multiple diffraction because all reciprocal-lattice vectors lie in the same plane.

Thus, under the considered conditions we have to obtain the four-wave case at the centre of the section topogram where one has to see a disturbance of the interference fringes of the two-beam case. It is of interest to search other multiple diffraction configurations which are realized at relatively small values of the azimuthal angle φ for a given wavelength value. We have found that for Mo $K\alpha$ radiation ($\lambda = 0.07093$ nm) and for the angle φ which is near to $\varphi_0 = 4.938 \times 10^{-3}$ rad the four-wave case is realized with the additional reflections $(-1, -3, -1)$ and $(5, -3, -1)$.

It is evident that for the angle φ which is near to $\varphi_0 = -4.938 \times 10^{-3}$ the four-wave case with the additional reflections $(-1, 3, -1)$ and $(5, 3, -1)$ is also realized in accordance with the crystal symmetry. These three cases of multiple diffraction were observed in the experiment for the crystal thickness $t =$ 1013 µm. The results of the experiment are presented in §4. The accuracy of the experiment is not high. Nevertheless, a disturbance of the interference fringes is clearly seen.

It is of interest to study a disturbance of the interference fringes by means of computer simulations for the ideal case when a slit width is infinitely small (much less than the crystal thickness t), and the distance from the source to the detector is infinitely long. We note that in the cases mentioned above a pure Laue case of diffraction is realized when all diffracted beams go out the crystal through the other surface. The section topograms are calculated by means of Fourier transformation over the polar angle θ after calculation of the two-dimensional angular dependence on the plane (θ, φ). As a result, we obtain a map of the intensity distribution of the $(4, 0, 0)$ reflection on the plane (x, φ). A correspondence to the real section topogram on the plane (x, y) is easily obtained through the relation $y = L\varphi$.

This relation is valid in the geometrical optics approximation for very long distance L. In the real laboratory experiment the slit and the source have a finite size; therefore the picture is smoothed over the slit size and the angular source size. On the other hand, if the distance $L < 10\,L_{\rm f}$, where $L_{\rm f} \propto t/\chi_0$ is the distance of diffraction focusing (Afanas'ev & Kon, 1977*b*,*c*), then a slight change of the experimental picture can arise compared to the angular theoretical dependence of intensity, as was shown in the work of Kohn & Toneyan (1986). Here $\chi_0 \simeq 3 \times 10^{-6}$ is the diffraction parameter [see equation (3)].

We use the method of calculation of the angular dependence of multiple diffraction in the Laue case which was first described in the work of Kon (1976*a*,*b*). If the plane wave with the wavevector $\mathbf{k}_0$ is incident on the crystal, then it is refracted inside the crystal, and the wavevector becomes $\mathbf{k}_0 + \varepsilon\mathbf{n}_0/2$. Because of diffraction of the wave on atomic planes of the crystal the additional waves arise with the wavevectors $\mathbf{k}_m + \varepsilon\mathbf{n}_0/2$, where $\mathbf{k}_m = \mathbf{k}_0 + \mathbf{h}_m$, $\mathbf{h}_m$ is the mth reciprocal-lattice vector of the considered configuration which satisfies the Bragg condition $k_m^2 = k_0^2$.

The electric field vector amplitude for the plane wave of the index m has two components in the plane normal to $\mathbf{k}_m$. Let us denote these components by the index s; then the scalar amplitudes are $\gamma_m^{-1/2} E_{ms}$. Here the parameter $\gamma_m = (\mathbf{k}_m \mathbf{n}_0)$ is used for convenience. The Maxwell equation for the total electric field inside the crystal is transformed to the set of equations for each component E_{ms}.

This set of equations can be written as an eigenvalue problem,

$$\sum_{ns'} G_{mn}^{ss'} E_{ns'} = \varepsilon E_{ms}, \tag{2}$$

for the scattering matrix G which has the form

$$G_{mn}^{ss'} = -\frac{K\alpha_m}{\gamma_m}\delta_{mn}\delta_{ss'} + \frac{K}{(\gamma_m\gamma_n)^{1/2}}\chi_{m-n}(\mathbf{e}_{ms}\mathbf{e}_{ns'}) \tag{3}$$

where the parameters $\alpha_m = (k_m^2 - k_0^2)/K^2$ depend on the angles θ and φ. The diffraction parameters χ_m are the complex values. They describe the amplitude of the kinematical scattering by the unit volume of the crystal. They were calculated using a program presented in the work of Kohn (2006*a*,*b*). The unit vectors of polarizations $\mathbf{e}_{ms}$ can be chosen to be arbitrary [for more details see Kon (1976*a*,*b*)].

The matrix G takes into account both the elastic scattering (the real part of the matrix G') and the absorption (the imaginary part of the matrix G''). In the Laue case the elements of the matrix G'' are always much less than the elements of the matrix G', which allows one to take them into account by means of the perturbation theory. In such an approach the eigenvalue problem is solved only for the real part that saves computer time. As a result we obtain $2N$ eigen solutions where N is the number of waves of multiple diffraction. Then the absorption coefficients are calculated by means of the formula

$$\mu_j = \varepsilon_j'' = \sum_{ms,ns'} E_{ms}^{(j)} (G'')_{mn}^{ss'} E_{ns'}^{(j)} \tag{4}$$

where the index j is used for various eigen solutions.

The total electric field of X-ray radiation is a superposition of all eigen solutions, each of them having a weight $\lambda_j(p)$ which is calculated from the boundary conditions and depends on the incident wave polarization index p. In the Laue case the boundary conditions are related only to the entrance surface and have the form

$$\sum_j \lambda_j(p) E_{ms}^{(j)} = (\gamma_0 I_e)^{1/2} \delta_{m0}\delta_{sp} \tag{5}$$

where I_e is the intensity of the incident wave.

Due to orthonormality of the eigen solutions the set of equations (5) can be easily solved, and the result is $\lambda_j(p) = (\gamma_0 I_e)^{1/2} E_{0p}^{(j)}$. Finally the reflection amplitude from the incident wave of the polarization p to the reflected wave of index m and the polarization s is equal to

$$R_m^{(p,s)}(\theta, \varphi) = \sum_j E_{0p}^{(j)} E_{ms}^{(j)} \exp(i\varepsilon_j t) \tag{6}$$

where t is the crystal thickness.

For the given reflection we have four complex values which depend on the angles θ and φ. If the incident radiation is the plane unpolarized wave, then for the calculation of the mth reflection coefficient it is sufficient to make a sum of square modulus of four values and multiply it by the factor 0.5 which is the weight of the various polarizations of the incident wave.

In our case of section topography one more step is necessary, namely, the Fourier transformation for the variable $q = K\theta$. So we need to calculate the four new values:

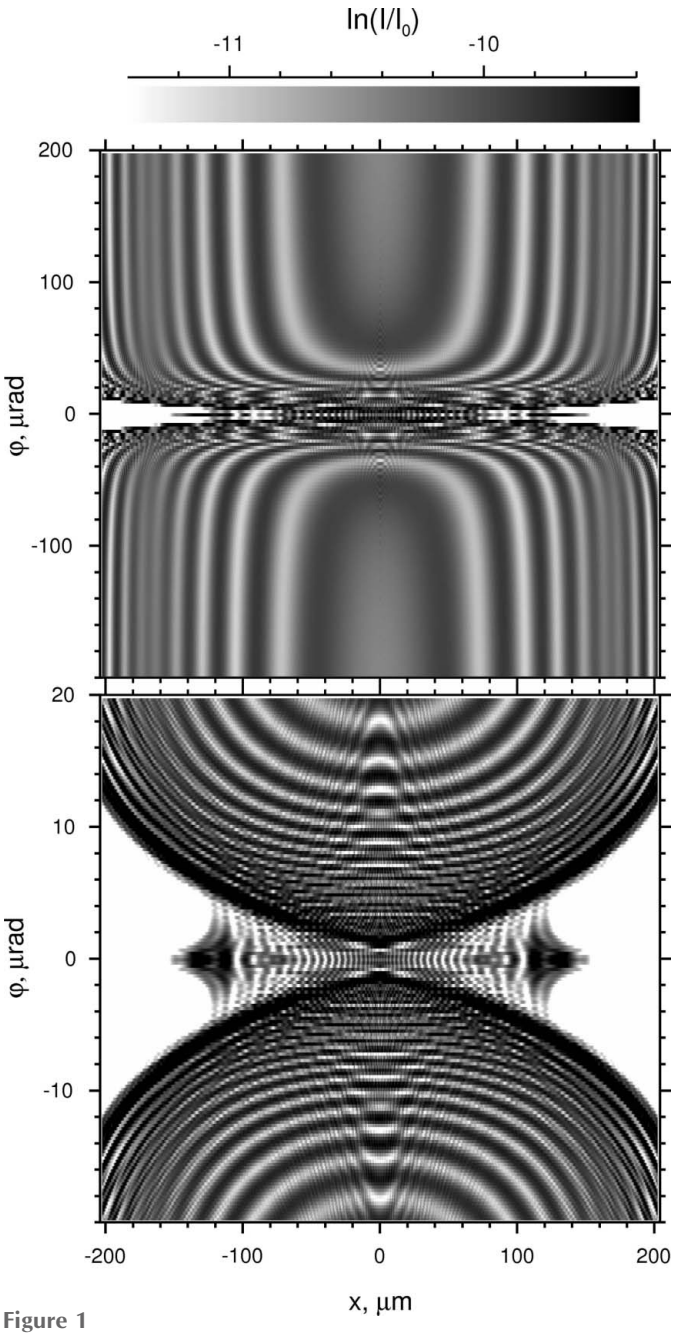

Figure 1
Computer simulation of a section topogram for the 400 reflection near the azimuthal angle $\varphi_0 = 0$. The intensity logarithm is shown. The top panel shows a large interval over φ where the inclination of the interference fringes of two-beam diffraction is clearly seen. The bottom panel shows the multiple diffraction area itself with a higher resolution over the azimuthal angle. The parameters are shown in the text.

$$U_m^{(p,s)}(x,\varphi) = \int \frac{dq}{2\pi} R_m^{(p,s)}(q,\varphi)\exp(iqx). \qquad (7)$$

This transformation is equivalent to the spherical wave theory of Kato (1961). We note that if the distance L_s between the slit and the detector is sufficiently long ($L_s > 0.1L_f$), then it is necessary to use more advanced theory developed in the work of Kon (1977*a*,*b*). The result is obtained as a half sum of square modulus $U_m^{(p,s)}$.

3. The results of calculations

Fig. 1 shows the multiple diffraction (0, 0, 0; 2, 2, 0; 4, 0, 0; 2, −2, 0) area at the centre of the section topogram (near the point $\varphi_0 = 0$) for the conditions discussed above, namely, the silicon crystal plate of thickness t = 1013 μm with the surface normal to the (0, 0, 1) direction, Mo $K\alpha$ radiation, (4, 0, 0) reflection. The horizontal size of the picture is four times less than the region of calculation and less than the base of the Borrmann triangle which is equal to $2t\sin\theta_B$ = 533 μm.

The top panel shows a large region over the azimuthal angle within the interval from −200 to 200 μrad. The contrast is shown with a linear scale of grey levels for the relative intensity logarithm, *i.e.* $\ln(I/I_0)$, within the interval from −11.4 to −9.4. Here I_0 is the intensity in the free-space case, *i.e.* without the slit and the crystal. The maximum is black, the minimum is white which is correspondent to the photoplate as a detector.

One can see that for large deviations of azimuthal angle from the multiple diffraction point the interference fringes are fully correspondent to the two-beam case. They are described by a sum of two functions (Afanas'ev & Kohn, 1971):

$$I_s(x) = \left|\frac{B_s}{4\cos\theta_B} J_0\left\{B_s[(t\sin\theta_B)^2 - x^2]\right\}\right|^2 \exp(-\mu t) \qquad (8)$$

where $B_s = K\chi_h C_s(2\sin\theta_B)^{-1}$, $\mu = K\chi_0''$ is a linear absorption coefficient, $J_0(z)$ is the Bessel function of zero order, χ_h and χ_0 are the Fourier images of the crystal susceptibility for the scattering on the reciprocal-lattice vector and the forward scattering, respectively. The factor C_s has two values 0 and $\cos(2\theta_B)$ for the two polarization states.

One can see that a sum of two pictures with different periods of oscillations leads to smoothing of some fringes because regions of intensity maximum for one picture correspond to regions of intensity minimum for another picture. This is a peculiarity of the unpolarized laboratory source. With decreasing distance to the multiple diffraction region the two-beam interference fringes become inclined, and then the picture becomes very complicated because new fringes appear with smaller periods and four polarization states.

It is of interest that at the centre of the multiple diffraction region the size of the Borrmann triangle becomes smaller and some focusing of almost all modes of radiation takes place with increasing intensity. Nevertheless, some modes are not focused. They form a separate interference structure.

The bottom panel shows the multiple diffraction area with a smaller step over the azimuthal angle. To observe this struc-

ture experimentally one has to have very high resolution over the azimuthal angle. For example, if the source size is equal to 20 μm, then for the resolution of 1 μrad it is necessary to have a distance of 20 m. The effect of compressing the beam is rather interesting. At present, it is difficult to propose some simple nature of such compression, and an additional study is necessary.

Fig. 2 shows the multiple diffraction (0, 0, 0; 4, 0, 0; 5, −3, −1; −1, −3, −1) area which arises first with increasing the azimuthal angle (near the point $\varphi_0 = 4.938 \times 10^{-3}$ rad). Once again the top panel shows a large region over the azimuthal angle within the interval from −400 to 400 μrad counted from the φ_0 value, and the bottom panel shows only the multiple diffraction area with a smaller step. The contrast of relative intensity logarithm is shown as in Fig. 1.

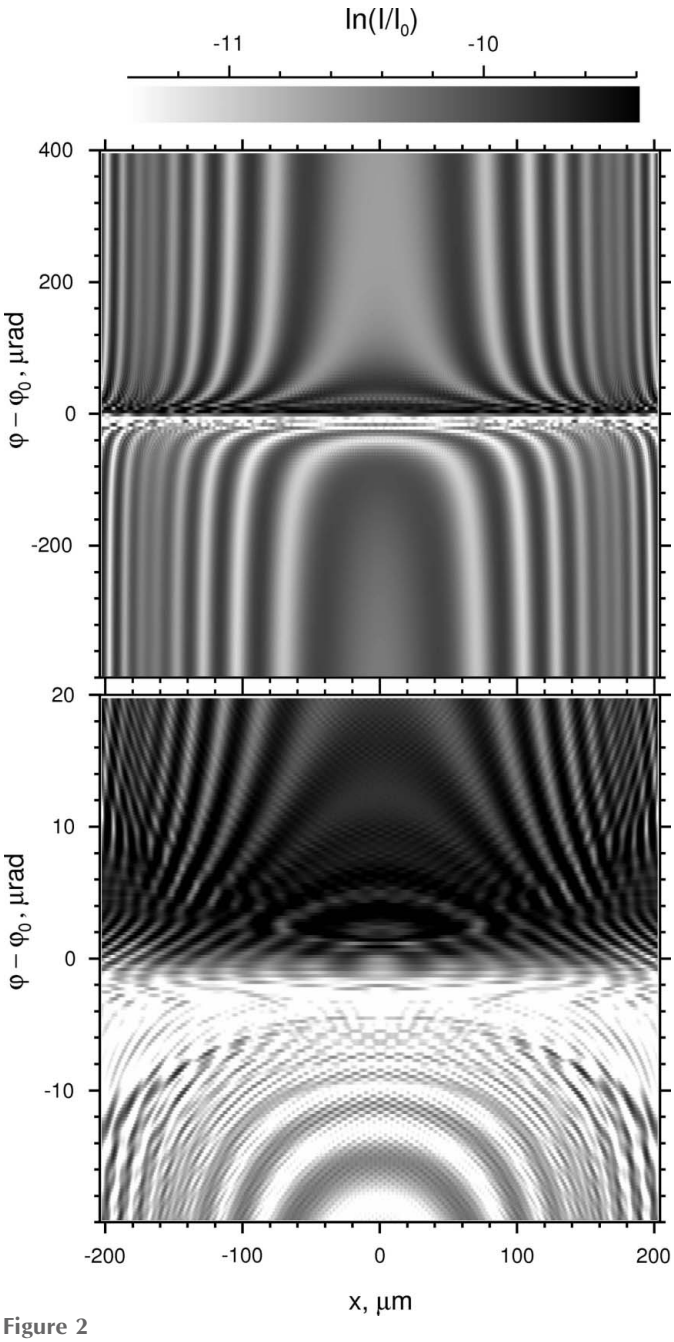

Figure 2
Computer simulation of a section topogram for the 400 reflection near the azimuthal angle $\varphi_0 = 4.9 \times 10^{-3}$ rad. The intensity logarithm is shown. The top panel shows a large interval over φ where the inclination of the interference fringes of two-beam diffraction is clearly seen. The bottom panel shows the multiple diffraction area itself with a higher resolution over the azimuthal angle. The parameters are shown in the text.

A peculiarity of this case is that both additional reciprocal-lattice vectors lie from one side relative to the vector 4, 0, 0 at the y axis. Correspondingly, the disturbance of the interference fringes is asymmetrical. For positive deviations over the azimuthal angle the fringe period increases, for negative deviations it decreases, and some fringes become semicircular.

The bottom panel allows one to understand that compressing the beam in this case takes place only for part of the radiation. Simultaneously new modes of the field appear for which the fringes have a smaller period without compressing the beam. It is of interest that with high resolution over the azimuthal angle the horizontal period of interference fringes can be experimentally registered because it is more than 10 μm. This period has to be compared with the slit size in front of the crystal, but not the source size.

4. The experimental results

The experimental setup is shown in Fig. 3. The laboratory source of Mo $K\alpha$ unpolarized radiation was used. The source focus sizes were 28 × 30 μm. The topograms were obtained with a Lang camera model A-3. The first slit has a size 400 μm and is located at a distance 55 mm from the source. The second slit has a size within the interval from 10 to 15 μm and is located at a distance 260 mm from the first slit. The sample was fixed at a distance 40 mm from the second slit. The distance from the sample to the photoplate was 15 mm. The third slit of size near to 1 mm was located directly in front of the photoplate. The size of the slit was almost two times larger than the base of the Borrmann triangle for the crystal of thickness 1013 μm. We note that the second slit restricts the beam very strongly, and it can be considered as the secondary source. The degree of coherence of such a secondary source can be characterized by the size of spatial coherence, see, for example, Born & Wolf (1999). This size is determined by the formula $L_{tc} = \lambda Z/w_s$, where λ is the radiation wavelength, Z is the distance from the source to the slit, w_s is the source transverse size. For the above experimental parameters we calculate L_{tc} = 0.8 μm which is much less than the size of the slit. So the slit can be considered as an incoherent source. The other reason

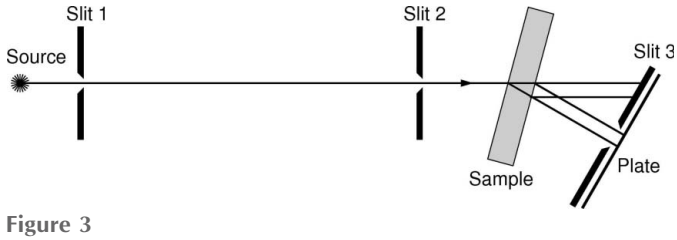

Figure 3
The experimental setup. The distances and sizes are described in the text.

for incoherence is the relative energy bandwidth ($\Delta E/E = 3 \times 10^{-4}$) of the radiation. Various values of wavelength are incoherent. The pictures for these are shifted relative to the slit. Therefore it is a good approximation to calculate the picture for the monochromatic source, and then to average the intensity distribution over the slit size.

As for the coordinate along the slit, effective averaging of the angular dependence has to be done over the angular source size $\Delta\varphi$. The latter is calculated as a ratio of the source size and the total distance from the source to the photoplate. In our case $\Delta\varphi = 8 \times 10^{-5}$. Fig. 4 shows the experimental pictures of the interference fringes of the 4, 0, 0 diffraction beam. The topogram width (along the X axis) is equal to the base of the Borrmann triangle 533 µm increased additionally by the slit size. The topogram length (along the Y axis) is more than 6 mm. The topogram shows all three cases of multiple diffraction discussed in the previous section. Various segments of the topogram along the Y axis correspond to various values of the azimuthal angle φ.

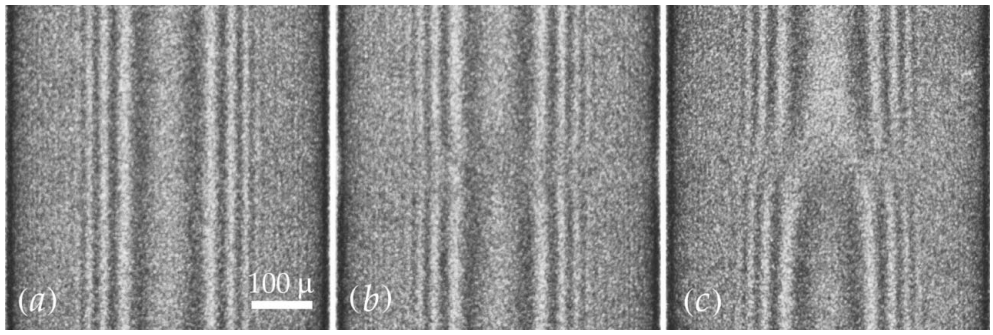

Figure 4
Fragments of the experimental section topogram. (*a*) Two-beam 400 diffraction in the silicon single crystal of thickness 1013 µm. (*b*) The multiple diffraction area near the azimuthal angle $\varphi_0 = 0$. (*c*) The multiple diffraction area near the azimuthal angle $\varphi_0 = 4.9 \times 10^{-3}$ rad.

The panel (*a*) of the figure shows a segment for such a value of φ where the effect of multiple diffraction is absent. Almost all the parts of the topogram seem like this segment. However, in some parts the interference fringes become different. First, this takes place at the centre of the topogram where $\varphi = 0$. This fragment is shown in the panel (*b*). Here the four-wave (0, 0, 0; 2, 2, 0; 4, 0, 0; 2, −2, 0) diffraction takes place. The panel (*c*) corresponds to the four-wave (0, 0, 0; 4, 0, 0; 5, −3, −1; −1, −3, −1) diffraction which takes place at φ near $\varphi_0 = 4.9 \times 10^{-3}$ rad. We note that the vertical size of the pictures (533 µm) corresponds to the interval of φ values as 1.5×10^{-3} rad.

Despite the very low resolution of the experimental topogram over the azimuthal angle, the fragment (*c*) shows clearly decreasing distance between light strips at the bottom part and increasing distance at the top part. As for the fragment (*b*), in this case the decrease in the distance takes place in both the top and bottom parts; therefore the effect is not clearly seen, but one can see the fact of fringe disturbance. The main problem of laboratory investigations of multiple diffraction by means of section topography consists of a low resolution over the azimuthal angle φ. On the other hand, the results of computer simulations show that the multiple diffraction area of the section topogram has a very complicated structure which is difficult to interpret within the simple theoretical model. The simplest property of multiple diffraction is a renormalization of the two-beam diffraction parameters by means of double diffraction through the additional reflections on the periphery of the multiple diffraction area which leads to the fringe inclination.

5. Conclusion

The method of computer simulation of the section topogram for a single crystal under conditions of multiple diffraction is developed in the Laue case. In a silicon single crystal with the surface normal to one of the main axes, the cases of multiple diffraction are found for very small values of azimuthal angle. They can be observed experimentally on the same topogram, *i.e.* without a rotation of the crystal. The results of calculations show that the multiple diffraction is seen on the section topogram in two different ways. First, in the centre of the multiple diffraction area the structure of interference fringes becomes very complicated, and a dependence on the azimuthal angle becomes very sharp. Secondly, on the periphery of the multiple diffraction area a weak change of the two-beam diffraction parameters leads to the characteristic inclination of the interference fringes.

The second phenomenon can be observed even in the experiment using a laboratory source of X-ray radiation under the conditions of low resolution over the azimuthal angle. The specific results are presented only for the reflection 400. However the effect of two-beam interference fringe disturbance for small values of the azimuthal angle was observed for the 220 and 800 reflections. The method of searching the additional reflections for any value of the azimuthal angle and any basic reflection is developed. The results of computer simulations are correspondent to our experimental topograms.

References

Afanas'ev, A. M. & Kohn, V. G. (1971). *Acta Cryst.* A**27**, 421–430.
Afanas'ev, A. M. & Kohn, V. G. (1977*a*). *Acta Cryst.* A**33**, 178–184.
Afanas'ev, A. M. & Kon, V. G. (1977*b*). *Fiz. Tverd. Tela (Leningrad)*, **19**, 1775–1783.
Afanas'ev, A. M. & Kon, V. G. (1977*c*). *Sov. Phys. Solid State*, **19**, 1035–1040.
Authier, A. (2005). *Dynamical Theory of X-ray Diffraction*, 3rd ed. Oxford University Press.
Born, M. & Wolf, E. (1999). *Principles of Optics*, 7th ed. Cambridge University Press.
Chang, S.-L. (2004). *X-ray Multiple-Wave Diffraction: Theory and Application. Springer Series in Solid-State Sciences*. Berlin: Springer.
Hart, M. & Lang, A. R. (1961). *Phys. Rev. Lett.* **7**, 120–121.

Heyroth, F., Höche, H.-R. & Eisenschmidt, C. (1999). *J. Appl. Cryst.* **32**, 489–496.
Høier, R. & Aanestad, A. (1981). *Acta Cryst.* A**37**, 787–794.
Høier, R. & Marthinsen, K. (1983). *Acta Cryst.* A**39**, 854–860.
Kato, N. (1961). *Acta Cryst.* **14**, 526–532.
Kato, N. & Lang, A. R. (1959). *Acta Cryst.* **12**, 787–794.
Kazimirov, A. & Kohn, V. G. (2010). *Acta Cryst.* A**66**, 451–457.
Kazimirov, A. & Kohn, V. G. (2011). *Acta Cryst.* A**67**, 409–414.
Kohn, V. G. (2006*a*). *Kristallografia (Moscow)*, **51**, 1001–1005.
Kohn, V. G. (2006*b*). *Crystallogr. Rep.* **51**, 729–733.
Kohn, V. G. & Kazimirov, A. (2012). *Acta Cryst.* A**68**, 331–336.
Kohn, V. G. & Toneyan, A. H. (1986). *Acta Cryst.* A**42**, 441–449.
Kon, V. G. (1976*a*). *Fiz. Tverd. Tela (Leningrad)*, **18**, 2538–2545.
Kon, V. G. (1976*b*). *Sov. Phys. Solid State*, **18**, 1482–1486.
Kon, V. G. (1977*a*). *Fiz. Tverd. Tela (Leningrad)*, **19**, 3567–3574.
Kon, V. G. (1977*b*). *Sov. Phys. Solid State*, **19**, 2085–2089.
Kon, V. G. (1988*a*). *Kristallografia (Moscow)*, **33**, 567–573.
Kon, V. G. (1988*b*). *Sov. Phys. Crystallogr.* **33**, 333–336.
Pinsker, Z. G. (1978). *Dynamical Scattering of X-rays in Crystals.* Heidelberg, New York: Springer-Verlag.
Renninger, M. (1937). *Z. Naturwiss.* **25**, 43.